

1 **Detrimental Effects of Nasal Microplastic Exposure on Normal and Asthmatic Pulmonary**  
2 **Physiology**

3 Kuo Lu<sup>1</sup>, Shuqin Ji<sup>2</sup>, Ziyi Lin<sup>2</sup>, Keng-Po Lai<sup>3</sup>, Shanze Chen<sup>1</sup>, Chen Qiu<sup>1\*</sup>, Lei Li<sup>2\*</sup>, Lingwei Wang<sup>1\*</sup>

4 **Affiliations**

5 1. Key Laboratory of Shenzhen Respiratory Disease, Shenzhen Institute of Respiratory Disease,  
6 The Second Clinical Medical College, Jinan University (Shenzhen People's Hospital),  
7 Shenzhen 518020, China; Post-doctoral Scientific Research Station of Basic Medicine, Jinan  
8 University, Guangzhou 510632, China.

9 2. Guangdong Provincial Key Laboratory of Brain Connectome and Behavior, CAS Key  
10 Laboratory of Brain Connectome and Manipulation, the Brain Cognition and Brain Disease  
11 Institute (BCBDI), Shenzhen Institutes of Advanced Technology, Chinese Academy of Sciences;  
12 Shenzhen-Hong Kong Institute of Brain Science-Shenzhen Fundamental Research Institutions,  
13 Shenzhen, 518055, China.

14 3. Guangxi Key Laboratory of Tumor Immunology and Microenvironmental Regulation, Guilin  
15 Medical University, Guilin, PR China

16 \*Corresponding authors. Email: (C. Q.) szchester@163.com, (L. L.) saralilei@siat.ac.cn, (L. W.)  
17 limey12@vip.sina.com

18  
19 **Abstract**

20 Concerns that airborne microplastics (MP) may have detrimental consequences on human health  
21 are rising. However, research on the effects of MP on the respiratory system are lacking. We tested  
22 the effect of MP exposure on both normal and asthmatic pulmonary physiology in mice. Our study  
23 shows that nasal MP exposure caused pulmonary inflammatory cell infiltration, bronchoalveolar  
24 macrophage aggregation, increased bronchoalveolar lavage fluid TNF- $\alpha$  level and plasma IgG1  
25 production in the normal mice. In an allergic asthma model, MP exposure also exacerbated asthma

26 symptoms, such as increased inflammatory cell infiltration with notable macrophage aggregation.  
27 Further Co-labelling of macrophage markers with MP particle incorporated fluorescence indicating  
28 the phagocytosis of the MP particles by bronchoalveolar macrophages. In summary, we show that  
29 MP exposure led to detrimental effects on the respiratory system in both healthy and asthmatic mice,  
30 which calls for urgent discourse and action to mitigate microplastic pollutants.

31 **Key words:** Microplastic, asthma, respiratory system, health risk

## 32 **Introduction**

33 Microplastic (MP) particles are a relatively recent type of environmental pollutant and have  
34 been detected in the air of densely populated cities (1). Synthetic fibers are the main source of  
35 airborne MP, which also includes pellets, films, fragments, and particles. The type and  
36 concentration of airborne MPs are affected by community lifestyle choices, human activities, and  
37 meteorological conditions (2, 3). Airborne MPs also reach and accumulate in remote areas and pose  
38 a threat to human health (4-6). Due to their small size, MPs in the air can be directly inhaled (3, 7)  
39 and are detected both in indoor and outdoor dust, and indoor dust is a considerable source of human  
40 MP exposure (8, 9).

41 Following inhalation of air pollutants, primary exposure occurs in the respiratory tract: the  
42 nasal passages down through the airways to the alveolar gas exchange units in the lungs represents  
43 the prime interface between the immune system and the airborne environment (10). Concerns that  
44 airborne microplastics (MP) may have detrimental consequences on human health are rising.  
45 However, research on the effects of MP on the respiratory system are lacking, especially in vivo  
46 mammalian studies.

47 Among all respiratory diseases, asthma currently affects 1-18% of the populations of different  
48 countries (11). Asthma symptoms appear to stem from a synergy of environmental and genetic  
49 factors (13). High amounts of particulate air pollution can cause pulmonary injury (14), and  
50 exposure to fine particulate matter, such as diesel exhaust particles and cigarette smoke, is

51 associated with frequency of asthmatic symptoms (10, 15-19). Whilst low levels of MP particles  
52 disrupts the normal pulmonary barrier *in vitro* (20), the effects of MPs on allergic asthma has not  
53 yet been studied. It is of great importance to determine the effects of MP exposure on the respiratory  
54 system of both healthy and asthmatic populations.

55 To explore the effect of MPs on both normal and asthmatic respiratory physiology, we  
56 developed a 24-day murine model of nasal MP exposure with a particle size of 1~5  $\mu\text{m}$ . To study  
57 its effects on asthma symptoms, a House Dust Mite (HDM)-induced allergic asthma model was  
58 also developed and subjected to nasal MP exposure as well. We examined the effects of MP  
59 exposure on inflammatory cells responses in the lungs, the bronchoalveolar lavage fluid  
60 inflammatory cytokines, airway mucus production, airway hyperresponsiveness, and total plasma  
61 immunoglobulin E (IgE) and immunoglobulin G1 (IgG1) production in normal and asthmatic mice.

62

## 63 **Results**

### 64 **Nasal MP exposure induces an increase of pulmonary inflammatory cells in normal mice and** 65 **aggravates HDM-induced airway inflammation in asthmatic mice**

66 An allergic asthma model was generated by HDM-sensitization and challenge as illustrated in  
67 Figure 1A. To investigate possible effects of nasal MP exposure on the development of HDM-  
68 induced allergic asthma, both control (normal) mice and asthmatic mice were exposed to a nasal-  
69 drip containing either MP or saline every other day for 24 days during allergen sensitization and  
70 challenge (Fig. 1A). As expected, the asthma group (Asthma+saline) had higher levels of eosinophil  
71 and lymphocytes in the bronchoalveolar lavage fluid (BALF) than the normal group when exposed  
72 only to saline (Normal+saline) ( $P<0.01$ ,  $t=4.270$ ,  $df=7$ ,  $P<0.01$ ,  $t=3.795$ ,  $df=7$ , Fig. 1B). Normal  
73 mice with MP exposure (Normal+MP) had higher BALF-eosinophil levels ( $P<0.05$ ,  $t=2.283$ ,  $df=9$ ,  
74 Fig. 1B) than normal mice with saline (Normal+saline), and a tendency towards higher neutrophil  
75 levels ( $P=0.0724$ ,  $t=2.035$ ,  $df=9$ ) and monocyte ( $P=0.2293$ ,  $t=1.290$ ,  $df=9$ , Fig. 1B) in BALF.

76 Asthmatic mice exposed to MP (Asthma+MP) had higher eosinophil, lymphocyte and neutrophil  
77 levels than the normal mice with saline (Normal+saline,  $P<0.01$ ,  $t=4.585$ ,  $df=9$ ;  $P<0.001$ ,  $t=6.586$ ,  
78  $df=9$ ;  $P<0.05$ ,  $t=2.704$ ,  $df=9$ , Fig. 1B). More importantly, the asthma group with MP exposure  
79 (Asthma+MP) had a greater inflammatory response than did the asthma with saline group, reflected  
80 by higher lymphocyte levels ( $P<0.05$ ,  $t=3.007$ ,  $df=8$ , Fig. 1B) and a trend towards higher eosinophil  
81 levels ( $P=0.0664$ ,  $t=2.124$ ,  $df=8$ , Fig. 1B).

82 The dramatically higher levels of inflammatory cells revealed by BALF cell counting were  
83 confirmed by H&E staining of lung tissue (Fig.1C). Massive inflammatory-cell infiltration can be  
84 seen in both Asthma+saline group and Asthma+MP groups. Different types of inflammatory cells  
85 were identified according to their histological features; namely, eosinophils, lymphocytes,  
86 neutrophils, plasmocytes and macrophages (Fig. S1).

87

### 88 **MP exposure results in an aggregation of macrophages and phagocytosis of MP particles by** 89 **macrophages in both normal and asthmatic mice**

90 It is intriguing that macrophages were present in the lung, as seen following H&E staining,  
91 and also that there was a trend towards higher monocytes after MP exposure. Considering the role  
92 of macrophages to phagocytize foreign materials, such as dust (19) and carbon particles (21) in the  
93 lung, we next performed immunohistochemical staining of macrophage markers in lung sections.  
94 The MP particles (1~5  $\mu\text{m}$ ) we used in this study was incorporated with green fluorophore, which  
95 appear a light-green color using bright-field microscopy, whilst emitting bright green fluorescence  
96 using fluorescence microscopy. Using an anti-Cluster of Differentiation 68 (CD68, a macrophage  
97 marker) antibody, we found co-labeling of CD68-positive brown DAB (3,3'-diaminobenzidine)  
98 staining with light-green colored MP particles in lung sections in both MP groups (Normal+MP  
99 and Asthma+MP) under a light microscope (Fig. 2A). This suggests possible macrophage-induced  
100 phagocytosis of MP particles. To confirm this, we used three different macrophage markers to

101 investigate possible co-localization with MP-particle fluorescence in three separate IHC  
102 experiments. The macrophage markers used were CD68, ionized calcium binding adaptor molecule  
103 1 (IBA-1) and Cluster of Differentiation 206 (CD206). Each macrophage marker showed a high  
104 percentage of colocalization with MP particles (Fig. 2B). Macrophages were observed inside and  
105 outside of bronchioles (Fig 2B, dotted lines indicate bronchiole lumen). Macrophage aggregation  
106 induced by MP exposure is illustrated by the representative images from all the four treatments in  
107 Figure 3A. Following quantification of macrophages in the lungs (Fig. 3B), we found that both MP  
108 groups had a higher amount of macrophages than the normal with saline group ( $P<0.01$ ,  $t=4.228$ ,  
109  $df=8$  for Normal+MP vs. Normal+saline;  $P<0.01$ ,  $t=4.137$ ,  $df=8$  for Asthma+MP vs. Normal+saline;  
110 Fig. 3B). Moreover, the asthma with MP group had considerably higher macrophage levels than  
111 the asthma with saline group ( $P<0.01$ ,  $t=3.519$ ,  $df=8$ ; Fig. 3B).

### 113 **MP exposure induces an increase in IgG1 production in both normal and asthmatic mice**

114 Considering the inflammation induced by MP exposure, we next investigated levels of IgE,  
115 IgG1 and inflammatory cytokines and found that the Asthma+saline group had higher levels of IgE  
116 ( $P<0.0001$ ,  $t=11.46$ ,  $df=14$ , Fig. 4A) and IgG1 ( $P<0.0001$ ,  $t=6.188$ ,  $df=14$ , Fig. 4A) compared with  
117 normal control group. MP exposure alone (Normal+MP) groups showed no increase in IgE levels  
118 while a dramatic increase in IgG1 levels ( $P<0.0001$ ,  $t=6.397$ ,  $df=14$ , Fig. 4A) compared with  
119 normal control group. Asthma+MP led to higher levels of both IgE ( $P<0.0001$ ,  $t=7.875$ ,  $df=14$ , Fig.  
120 4A) and IgG1 ( $P<0.0001$ ,  $t=5.792$ ,  $df=14$ , Fig. 4A) compared with Normal+saline group. However,  
121 no synergistic effect was observed with asthma and MP (i.e., neither Asthma+saline vs.  
122 Asthma+MP nor Normal+MP vs. Asthma+MP had different levels of IgE or IgG1).

123  
124 **Asthmatic mice showed elevated Th2-cytokine expression patterns whilst MP exposure**  
125 **induced an increase in Th1 type tumor necrosis factor- $\alpha$  increase in BALF**

126 Inflammatory cytokine levels in BALF were then measured using a Multiplex ELISA assay  
127 (Fig. 4B). Without MP exposure, we found higher levels of T helper type 2 (Th2) cytokines  
128 interleukin (IL)-4, IL-5 and IL-13 in the asthmatic mice than in controls (Asthma+saline vs.  
129 Normal+saline), which is typical in HDM-induced asthma mouse models ( $P<0.05$ ,  $t=2.325$ ,  $df=20$ ,  
130 for IL-4;  $P<0.05$ ,  $t=2.684$ ,  $df=20$ , for IL-5;  $P<0.01$ ,  $t=3.015$ ,  $df=20$ , for IL-13), whilst no such  
131 expression pattern was observed for Th1 or Th17 cytokines (Fig. 4B). Similarly, MP exposure  
132 coupled with asthma led to higher levels of IL-4, IL-5 and IL-13 than the normal with saline control  
133 group ( $P<0.05$ ,  $t=2.236$ ,  $df=21$ , for IL-4,  $P<0.05$ ,  $t=2.285$ ,  $df=21$ , for, IL-5 and  $P<0.01$ ,  $t=2.899$ ,  
134  $df=21$ , for IL-13), although no synergistic effect was observed MP exposure to asthmatic mice (no  
135 differences between Asthma+MP vs. Asthma+saline or Asthma+MP vs. Normal+MP, Fig. 4B).  
136 Exposure to MP in normal mice led to a statistically significant increase in tumor necrosis factor- $\alpha$   
137 (TNF- $\alpha$ ) level (Normal+MP vs Normal+saline,  $P<0.05$ ,  $t=2.674$ ,  $df=23$ ) whereas no effect on Th2  
138 cytokine expression levels were observed (Fig. 4B). Inflammatory cytokine levels from plasma  
139 were also measured, and higher levels of IL-5 were found in both asthma groups (Asthma+saline,  
140 Asthma+MP), than in the normal with saline control group (Fig. S2).

141

142 **There was no effect of MP exposure on airway mucus production or airway**  
143 **hyperresponsiveness**

144 In addition to pulmonary inflammation, we also investigated whether there was any effect of  
145 MP exposure on mucus production and airway hyperresponsiveness or a possible synergic effect of  
146 MP with allergic asthma in this aspect. We found that, without MP exposure, the asthma with saline  
147 group had higher amount of mucus production than the normal with saline group ( $P<0.01$ ,  $t=4.278$ ,  
148  $df=6$ ). There was no difference in mucus production attributable to MP exposure alone  
149 (Normal+MP vs. Normal+saline,  $P=0.1157$ ,  $t=1.838$ ,  $df=6$ , Fig 5A,B), and the asthma with MP  
150 group had a non-significant tendency toward higher mucus production than the asthma with saline

151 control ( $P=0.0739$ ,  $t=2.162$ ,  $df=6$ , Fig. 5A,B). To determine the effect of MP exposure on airway  
152 hyperresponsiveness, we used specific airway resistance (sRaw) in conscious mice (Fig. 6A-B).  
153 Our results showed that, without MP exposure, the asthma with saline group had a higher level of  
154 airway hyperresponsiveness than the normal with saline group, induced at 25 mg/ml, 50 mg/ml and  
155 100 mg/ml methacholine (Mch) stimulation ( $P<0.05$ ,  $t=3.326$ ,  $df=7$ ,  $P<0.05$ ,  $t=2.445$ ,  $df=7$ ,  $P<0.05$ ,  
156  $t=2.737$ ,  $df=7$ , Fig. 6B). Although the increase in airway hyperresponsiveness was not statistically  
157 significant following MP exposure or MP exposure to asthmatic mice, there was a trend towards  
158 higher airway hyperresponsiveness following high concentration of 100 mg/mg Mch stimulation  
159 ( $P=0.0572$ ,  $t=2.180$ ,  $df=9$  for Normal+MP vs. Normal+saline;  $P=0.0534$ ,  $t=2.222$ ,  $df=9$  for  
160 Asthma+MP vs. Normal+saline).

161

## 162 **Discussion**

163 In our study, we demonstrated that exposure to nasal microplastics (MP) induced elevated  
164 inflammation, such as macrophage aggregation, and had detrimental effects on both normal  
165 pulmonary physiology and asthma symptoms. Our study shows that nasal MP exposure caused  
166 inflammatory cell infiltration, macrophage aggregation, IgG1 production and TNF- $\alpha$  secretion in  
167 the lungs of normal mice. MP exposure also exacerbated asthma symptoms, such as increased  
168 inflammatory cell infiltration with notable macrophage aggregation.

169 The observation of co-labeling of MP particles and macrophages in our IHC staining was of  
170 particular interest. To confirm that the clustered MP particles were truly inside the macrophages,  
171 we used green-fluorescence-labeled MP particles and stained lung sections with three different  
172 antibodies to macrophages with a red-fluorescence, in three separate batches of experiments. We  
173 found distributions of macrophages co-labeled with MP particles both inside and outside  
174 bronchioles. This suggests the phagocytosis of MP particles by macrophages. Macrophages in  
175 mouse lungs are responsible for ingestion and clearance of inhaled particles and play a critical role

176 in the defense against pathogens, coordination of the adaptive immune response, and regulation of  
177 inflammation and tissue repair (22, 23). For example, exposure to diesel exhaust particles activates  
178 alveolar macrophages (24). The route of MP particles may break the pulmonary epithelium barriers  
179 by macrophages in the bronchioles phagocytizing the foreign MP particles then get outside of the  
180 bronchioles might be the route of how MP particles break the pulmonary barriers, get inside of the  
181 pulmonary tissues and even get accessed to other sites of the animal body.

182 We also found that macrophage activation is associated with increased production of TNF- $\alpha$ ,  
183 which is a potent mediator of inflammatory and immune responses. Elevated production of TNF- $\alpha$   
184 by activated macrophages has been associated with pulmonary inflammation (25) and the number  
185 of macrophages is associated with TNF- $\alpha$  release in response to exposure to diesel exhaust particles  
186 (24, 26).

187 MP exposure also increased the eosinophil levels in BALF. Eosinophils are the terminal  
188 effector cells and active regulators of Th2-type immune responses in the pathogenesis of asthma  
189 (27) and play an important role in response to allergen insults. They are known to induce T-cell  
190 proliferation and promote the recruitment of effector T cells to the lung (28, 29). Eosinophil  
191 deficiency results in reduction of Th2 immune responses occurring in respiratory inflammation  
192 mouse models (30). In turn, eosinophilia is driven by Th2 cytokines (e.g., IL-4, IL-5, IL-13), in  
193 particular by IL-5, which is a critical cytokine mediating increased eosinophil differentiation,  
194 maturation, activation, and survival (31). The BALF and plasma levels of IL-5 in the MP exposure  
195 asthmatic mice were both higher than those of the normal mice with saline group.

196 In our study, the MP particles of the size 1~5  $\mu\text{m}$  did not affect airway hyperresponsiveness.  
197 Actually, fine particle pollutants have been reported with various results with respect to airway  
198 hyperresponsiveness. For example, Wang et al. reported that particular matter < 2.5  $\mu\text{m}$  (PM2.5)  
199 led to increased airway resistance in asthmatic mice (32). Similarly, Ellen et al. showed that  
200 cigarette smoke increases airway hyperresponsiveness in asthmatic mice (18). However, Kaoru et



201 al. found that air-pollutant aerosol did not affect airway hyperresponsiveness in asthmatic mice (14)  
202 and Botelho et al. reported that cigarette smoke affects eosinophil migration without affecting  
203 airway resistance (33). The disparities between these results may be due to a host of factors,  
204 including the different nature of the pollutants, different animal species used, sex, different  
205 exposure protocols used and different allergens used to induce asthma models (18, 34).

206 To the best of our knowledge, this is the first in vivo study to investigate the effects of MP  
207 exposure on lung function of normal and asthmatic mice. The detrimental effect on normal lung  
208 physiology and the synergic effect of MP exposure and asthma calls for urgent discourse and action  
209 to mitigate microplastic pollutants, especially those with a diameter of 1~5  $\mu\text{m}$ . Due to the limitation  
210 of this single study, many interesting and important questions remain, such as: (i) the dose- and  
211 time-dependent effects of micrometer-sized MP exposure, (ii) the signaling pathway of macrophage  
212 phagocytosis of MP particles and possible follow-up transportation and effects of MP particles in  
213 the lung and other organs/tissues, and (iii) the effects of nanometer-sized MP (nanoplastics) on lung  
214 function in normal and asthma models.

## 216 **Materials and Methods**

### 217 **HDM-asthma model and microplastic treatment**

218 All husbandry and experimental procedures in this study were approved by the Scientific  
219 Research Ethics Committee of the Shenzhen People's Hospital and Shenzhen Institutes of  
220 Advanced Technology, Chinese Academy of Sciences. Adult (6~8 weeks old) female Balb/c mice  
221 (Beijing HFK Bioscience Co., Ltd, Beijing, China) were used in this study. Mice were housed in a  
222 12-hour light/dark cycle with unrestricted access to food and water.

223 A House Dust Mite (HDM) induced allergic asthmatic mouse model was established as  
224 previously described [1]. Mice were sensitized by subcutaneous injection of HDM (30  $\mu\text{g}$  in 100  
225  $\mu\text{L}$  saline) on day 0, 7, 14 using HDM extract (*Dermatophagoides pteronyssinus*, Wolcavi Biotech

226 Co., Ltd., Beijing, China). After 7 days of recovery, mice were then challenged daily (day 21 to day  
227 25) with intranasal administration of HDM (30 µg in 20µL saline) under light isoflurane anesthesia.  
228 On day 26, airway hyperresponsiveness (AHR) was determined before sacrifice.

229 To assess the effect of microplastics exposure on normal and HDM-induced allergic asthmatic  
230 mice, microplastic (FMG-Green Fluorescent Microspheres, 1.3 g/cc 1~5 µm, Cospheric, California,  
231 USA) were suspended in saline and administered intranasally (300 µg MP in 20 µL saline) from  
232 day 0 to day 24 every other day. Age- and gender-matched control mice were treated identically  
233 but with 20 µL saline. Four groups were included in the experimental set-up: Normal with saline,  
234 HDM-induced asthma with saline, Normal with MP exposure and HDM-induced asthma with MP  
235 exposure.

236

### 237 **Bronchoalveolar lavage fluid (BALF) and plasma collection and analysis**

238 Bronchoalveolar lavage was performed by cannulation of the trachea where lungs were rinsed  
239 three times with 0.5 mL PBS. The collected BALF was centrifuged at 1500 rpm, 4 °C for 10 min.  
240 The supernatant was subjected to Multiplex ELISA of inflammatory cytokines. The cell pellets  
241 were resuspended in PBS and the number of eosinophils, neutrophils, lymphocytes and monocytes  
242 were counted using a Sysmex XN-1000 analyzer (Sysmex Corporation, Kobe, Japan). The whole  
243 blood was collected from the mouse pericardium and placed in an anticoagulation tube containing  
244 EDTA-K2. Blood samples were centrifuged at 3000 rpm, 4 °C for 10 min to get the plasma.

245

### 246 **Histological analysis of H&E and PAS staining**

247 After completion of experiments, mice were anesthetized and transcardially perfused with 4%  
248 paraformaldehyde in PBS. Fixed lungs were subsequently rinsed in PBS, placed in the cassettes  
249 and embedded in paraffin or prepared for frozen sectioning. The paraffin blocks were obtained  
250 using a Multi-function embedding machine (Peisijie BM450A, China) and were sliced into 4-µm

251 sections using a microtome (SELL Cut5062, Germany) and then deparaffinized, hydrated, and  
252 stained. For paraffin sections, haematoxylin and eosin (H&E) staining, periodic acid Schiff (PAS)  
253 staining and immunofluorescent (IF) staining were performed. H&E was used to assess lung tissue  
254 histology and PAS staining was used to assess airway mucus production (KGA222, Jiangsu  
255 KeyGEN BioTECH Corp., Ltd, China). IF staining was used to identify the pulmonary cells with  
256 MP particles inside. Quantification of immunohistochemical staining and PAS positive staining  
257 was measured by NIH Image J software and PAS staining was further normalized using the  
258 perimeter of the airway basement membrane (27).

259

### 260 **Immunohistochemistry (IHC) and immunofluorescent staining**

261 The fixed lungs for frozen sectioning were immersed in a solution of sucrose (30% m/v in  
262 PBS) for 48 h and were then embedded in O.C.T. compound. Lung sections of 7  $\mu$ m were obtained  
263 using a cryostat microtome (Lecia CM1860, Germany) and stored at -20°C for  
264 immunohistochemical staining of a macrophage marker - CD68. We used the following reagents for  
265 IHC staining: rabbit anti-CD68 (1:100, Abcam, ab125212, UK), HRP-Polymer anti-Rabbit IHC Kit  
266 (MAX Vision, KIT-5004, China) and DAB (Maixin-Bio, DAB-0031, China) for visualization. The  
267 MP particles appear light green under a light microscope whilst the positive staining of CD68,  
268 stained by DAB, appear a brown color.

269 The paraffin sections underwent immunofluorescent staining of macrophage markers CD68,  
270 IBA-1 and CD206 separately. First, paraffin sections were dried in a 65 °C oven for 2 h, dewaxed  
271 to water, and then washed three times for 5 min with PBS. The slices were placed in EDTA buffer  
272 for microwave repair. After bringing to the boil using a low power microwave setting, power was  
273 turned off for 10 min, then heated on low-power until boiling. Slices were then washed 3 times with  
274 PBS after cooling to room temperature, placed in 3% hydrogen peroxide solution and incubated at  
275 room temperature in the dark for 10 min. The slices were washed 3 times for 5 min with PBS, and

276 then blocked with 5% BSA for 20 min. The blocked tissues were incubated with diluted primary  
277 antibody overnight at 4 °C and then washed again three times for 5 min with PBS. Then, 50 µL of  
278 the appropriate secondary antibody was added prior to incubation at 37 °C for 50 min followed by  
279 three 5-min PBS washes. Then, 50 µL DAPI staining solution was added to each section, and  
280 incubated at room temperature in darkness for 5 min. After staining, sections were given three 5-  
281 min PBS washes. Next, an appropriate amount of antifading reagent (Polyvinyl alcohol mounting  
282 medium with DABCO, SIGMA-ALDRICH Co., St. Louis, USA) was dropped onto the tissues,  
283 then cover-slipped, and observed under a fluorescent microscope. Primary antibodies for  
284 immunofluorescent staining were prepared as follows: rabbit anti-CD68 (1:100, servicebio,  
285 Gb11067, China), rabbit anti-IBA-1 (1:150, Abcam, Ab178847, UK), rabbit anti-CD206 (1:100,  
286 Abcam, Ab64693, UK). Secondary antibody used was Alexa Fluor 594 goat anti-rabbit (1:50,  
287 Aspen, AS-1109, USA). The slices were observed under an inverted microscope IX51 (Olympus,  
288 Japan) and analyzed by the MicroPublisher Q-IMAGING system (Q-Imaging, Canada). The MP  
289 particles (1~5 µm) we used in this study was incorporated with green fluorophore, emitting bright  
290 green fluorescence using fluorescence microscopy The MP particles incorporated with green  
291 fluorophore emitting bright green fluorescence whilst the positive staining of macrophage markers  
292 emitting red fluorescence.

293

#### 294 **Multiplex ELISA and IgE / IgG1 ELISA**

295 Cytokine concentration was measured in cell-free supernatants of BALF and plasma. We used  
296 the multiplex ELISA (MERK-Millipore, cat. no. MTH17MAG-47K-08, Millipore Co., Billerica,  
297 USA) for simultaneous quantification of the following 8 analytes in the mouse BALF and plasma  
298 samples: IL-4, IL-5, IL-10, IL-13, IL-17A, IL-33, IFN- $\gamma$  and TNF- $\alpha$ . An analyzer (Instrument  
299 Luminex 200TM, Luminex Corporation, Austin, USA) was used to acquire and analyze data.  
300 Plasma was collected from mouse blood samples and the amount of total IgE and IgG1 were

analyzed using RayBio mouse IgE ELISA Kits (RayBio, cat. ELM-IgE, Ray Biotech, Inc., Norcross, USA) and Solarbio IgG1 ELISA Kits (Solarbio, cat. SEKM-0097, Beijing Solarbio Science & Technology Co., Ltd., Beijing, China) according to the manufacturer instructions.

### **Airway hyperresponsiveness (AHR)**

Specific airway resistance (sRaw) in conscious mice was assessed using FinePointe™ Non-Invasive Airway Mechanics chambers (Buxco Electronics, Inc., Wilmington, North Carolina) according to a previously described method (35, 36). This used double-flow plethysmography that calculated sRaw by analyzing breathing patterns at nasal and thoracic airflows. For the determination of sRaw in mice, inhalations of saline and methacholine were administered. Aerosols were delivered into the nasal cavity for 30 s in a dose-response manner: 0 (saline), 6.25, 12.5, 25, 50 and 100 mg of methacholine per milliliter. All measurements were made in an air-conditioned environment controlled for temperature (22 °C to 23 °C) and humidity (50% to 60%).

### **Statistical analysis**

Statistical analyses were carried out using PRISM software version 8.2 (GraphPad Software Inc, La Jolla, CA). Unpaired t test was used as appropriate and a *P* value <0.05 was considered significant. All n values represent the number of mice used in each experiment.

### **References**

1. S. L. Wright, J. Ulke, A. Font, K. L. A. Chan, F. J. Kelly, Atmospheric microplastic deposition in an urban environment and an evaluation of transport. *Environ. Int.* **136**, 1-7 (2020).
2. O. Mbachu, G. Jenkins, C. Pratt, P. Kaparaju, A New Contaminant Superhighway? A Review of Sources, Measurement Techniques and Fate of Atmospheric Microplastics. *Water Air Soil Pollut.* **231**, 1-27 (2020).

- 327 3. G. L. Chen, Q. Y. Feng, J. Wang, Mini-review of microplastics in the atmosphere and their  
328 risks to humans. *Sci. Total Environ.* **703**, 1-6 (2020).
- 329 4. Y. L. Zhang, T. G. Gao, S. C. Kang, M. Sillanpaa, Importance of atmospheric transport for  
330 microplastics deposited in remote areas. *Environ. Pollut.* **254**, 1-4 (2019).
- 331 5. S. Allen, D. Allen, V. R. Phoenix, G. Le Roux, P. D. Jimenez, A., Atmospheric transport  
332 and deposition of microplastics in a remote mountain catchment. *Nat. Geosci.* **12**, 339-344  
333 (2019).
- 334 6. N. Evangeliou, H. Grythe, Z. Klimont, C. Heyes, S. Eckhardt, S. Lopez-Aparicio, A. Stohl,  
335 Atmospheric transport is a major pathway of microplastics to remote regions. *Nat. Commun.*  
336 **11**, 1-11 (2020).
- 337 7. A. T. Kaya, M. Yurtsever, S. C. Bayraktar, Ubiquitous exposure to microfiber pollution in  
338 the air. *Eur. Phys. J. Plus* **133**, 1-9 (2018).
- 339 8. J. J. Zhang, L. Wang, K. Kannan, Microplastics in house dust from 12 countries and  
340 associated human exposure. *Environ. Int.* **134**, 1-7 (2020).
- 341 9. C. G. Liu, J. Ji, Y. L. Zhang, L. Wang, J. Deng, Y. Gao, L. Yu, J. J. Zhang, H. W. Sun,  
342 Widespread distribution of PET and PC microplastics in dust in urban China and their  
343 estimated human exposure. *Environ. Int.* **128**, 116-124 (2019).
- 344 10. D. A. Glencross, T.-R. Ho, N. Camilla, C. M. Hawrylowicz, P. E. Pfeffer, Air pollution and  
345 its effects on the immune system. *Free Radic. Biol. Med.* **151**, 56-68 (2020).
- 346 11. GINA Executive and Science committee. Global strategy for asthma management and  
347 prevention. 2020. [https://ginasthma.org/wp-content/uploads/2020/06/GINA-2020-  
348 report\\_20\\_06\\_04-1-wms.pdf](https://ginasthma.org/wp-content/uploads/2020/06/GINA-2020-report_20_06_04-1-wms.pdf).
- 349 12. T. S. Eisenman, S. P. Jariwala, G. S. Lovasi, Urban trees and asthma: a call for  
350 epidemiological research. *Lancet Resp. Med.* **7**, E19-E20 (2019).

- 351 13. K. Hufnagl, I. Pali-Scholl, F. Roth-Walter, E. Jensen-Jarolim, Dysbiosis of the gut and lung  
352 microbiome has a role in asthma. *Semin. Immunopathol.* **42**, 75-93 (2020).
- 353 14. K. Hamada, C. A. Goldsmith, A. Goldman, L. Kobzik, Resistance of very young mice to  
354 inhaled allergen sensitization is overcome by coexposure to an air-pollutant aerosol. *Am. J.*  
355 *Respir. Crit. Care Med.* **161**, 1285-1293 (2000).
- 356 15. Z. Celebi Sozener, L. Cevhertas, K. Nadeau, M. Akdis, C. A. Akdis, Environmental factors  
357 in epithelial barrier dysfunction. *J. Allergy Clin. Immunol.* **145**, 1517-1528 (2020).
- 358 16. B. Q. Zuo *et al.*, Associations between short-term exposure to fine particulate matter and  
359 acute exacerbation of asthma in Yancheng, China. *Chemosphere* **237**, 1-6 (2019).
- 360 17. L. Wang, J. Y. Xu, H. Liu, J. Li, H. L. Hao, PM2.5 inhibits SOD1 expression by up-  
361 regulating microRNA-206 and promotes ROS accumulation and disease progression in  
362 asthmatic mice. *Int. Immunopharmacol.* **76**, 1-12 (2019).
- 363 18. E. A. Lanckacker, K. G. Tournoy, H. Hammad, G. Holtappels, B. N. Lambrecht, G. F. Joos,  
364 T. Maes, Short cigarette smoke exposure facilitates sensitisation and asthma development  
365 in mice. *Eur. Resp. J.* **41**, 1189-1199 (2013).
- 366 19. E. B. Brandt, M. B. Kovacic, G. B. Lee, A. M. Gibson, T. H. Acciani, T. D. Le Cras, P. H.  
367 Ryan, A. L. Budelsky, G. K. Khurana Hershey, Diesel exhaust particle induction of IL-17A  
368 contributes to severe asthma. *J. Allergy Clin. Immunol.* **132**, 1194-1204 (2013).
- 369 20. C. D. Dong, C. W. Chen, Y. C. Chen, H. H. Chen, J. S. Lee, C. H. Lin, Polystyrene  
370 microplastic particles: In vitro pulmonary toxicity assessment. *J. Hazard. Mater.* **385**, 1-8  
371 (2019).
- 372 21. T. Terashima, B. Wiggs, D. English, J. C. Hogg, S. F. van Eeden, Phagocytosis of small  
373 carbon particles (PM10) by alveolar macrophages stimulates the release of  
374 polymorphonuclear leukocytes from bone marrow. *Am. J. Respir. Crit. Care Med.* **155**,  
375 1441-1447 (1997).

- 376 22. J. Bousquet, P. K. Jeffery, W. W. Busse, M. Johnson, A. M. Vignola, Asthma - From  
377 bronchoconstriction to airways inflammation and remodeling. *Am. J. Respir. Crit. Care Med.*  
378 **161**, 1720-1745 (2000).
- 379 23. J. Y. Hong, Y. Chung, J. Steenrod, Q. Chen, J. Lei, A. T. Comstock, A. M. Goldsmith, J. K.  
380 Bentley, U. S. Sajjan, M. B. Hershenson, Macrophage activation state determines the  
381 response to rhinovirus infection in a mouse model of allergic asthma. *Respir. Res.* **15**, 1-15  
382 (2014).
- 383 24. R. M. Kafoury, M. C. Madden, Diesel exhaust particles induce the over expression of tumor  
384 necrosis factor-alpha (TNF-alpha) gene in alveolar macrophages and failed to induce  
385 apoptosis through activation of nuclear factor-kappaB (NF-kappaB). *Int. J. Environ. Res.*  
386 *Public Health* **2**, 107-113 (2005).
- 387 25. K. E. Driscoll, D. G. Hassenbein, J. M. Carter, S. L. Kunkel, T. R. Quinlan, B. T. Mossman,  
388 TNF alpha and increased chemokine expression in rat lung after particle exposure. *Toxicol.*  
389 *Lett.* **82-83**, 483-489 (1995).
- 390 26. H.-M. Yang, J. Y. C. Ma, V. Castranova, J. K. H. Ma, Effects of Diesel Exhaust Particles  
391 on the Release of Interleukin-1 and Tumor Necrosis Factor-Alpha from Rat Alveolar  
392 Macrophages. *Exp. Lung Res.* **23**, 269-284 (1997).
- 393 27. J. Kim, S. Natarajan, L. J. Vaickus, J. C. Bouchard, D. Beal, W. W. Cruikshank, D. G.  
394 Remick, Diesel Exhaust Particulates Exacerbate Asthma-Like Inflammation by Increasing  
395 CXC Chemokines. *Am. J. Pathol.* **179**, 2730-2739 (2011).
- 396 28. E. A. Jacobsen, K. R. Zellner, D. Colbert, N. A. Lee, J. J. Lee, Eosinophils Regulate  
397 Dendritic Cells and Th2 Pulmonary Immune Responses following Allergen Provocation. *J.*  
398 *Immunol. Res.* **187**, 6059-6068 (2011).



- 399 29. E. R. Walsh, N. Sahu, J. Kearley, E. Benjamin, B. H. Kang, A. Humbles, A. August, Strain-  
400 specific requirement for eosinophils in the recruitment of T cells to the lung during the  
401 development of allergic asthma. *J. Exp. Med.* **205**, 1285-1292 (2008).
- 402 30. E. A. Jacobsen, N. A. Lee, J. J. Lee, Re-defining the unique roles for eosinophils in allergic  
403 respiratory inflammation. *Clin. Exp. Allergy* **44**, 1119-1136 (2014).
- 404 31. I.-S. Ok, S.-H. Kim, B.-K. Kim, J.-C. Lee, Y.-C. Lee, Pinellia ternata, Citrus reticulata, and  
405 Their Combinational Prescription Inhibit Eosinophil Infiltration and Airway  
406 Hyperresponsiveness by Suppressing CCR3+and Th2 Cytokines Production in the  
407 Ovalbumin-Induced Asthma Model. *Mediat. Inflamm.* **2009**, 1-11 (2009).
- 408 32. L. Wang, J. Xu, H. Liu, J. Li, H. Hao, PM2.5 inhibits SOD1 expression by up-regulating  
409 microRNA-206 and promotes ROS accumulation and disease progression in asthmatic mice.  
410 *Int. Immunopharmacol.* **76**, 1-12 (2019).
- 411 33. F. M. Botelho, A. Llop-Guevara, N. J. Trimble, J. K. Nikota, C. M. T. Bauer, K. N. Lambert,  
412 S. Kianpour, M. Jordana, M. R. Staempfli, Cigarette Smoke Differentially Affects  
413 Eosinophilia and Remodeling in a Model of House Dust Mite Asthma. *Am. J. Respir. Cell*  
414 *Mol. Biol.* **45**, 753-760 (2011).
- 415 34. V. L. Mitchell, L. S. Van Winkle, L. J. Gershwin, Environmental Tobacco Smoke and  
416 Progesterone Alter Lung Inflammation and Mucous Metaplasia in a Mouse Model of  
417 Allergic Airway Disease. *Clin. Rev. Allergy Immunol.* **43**, 57-68 (2012).
- 418 35. C. Fu, H. Lu, X. Wu, J. Liu, C. Liu, Z. Liu, W. Yuan, J. Zhou, S. Li, Chronic intermittent  
419 hypoxia decreases pulmonary clearance of <sup>99m</sup>Tc-labelled particulate matter in mice. *Am. J.*  
420 *Transl. Res.* **9**, 3060-3072 (2017).
- 421 36. N. Zang, J. Zhuang, Y. Deng, Z. Yang, Z. Ye, X. Xie, L. Ren, Z. Fu, Z. Luo, F. Xu, E. Liu,  
422 Pulmonary C Fibers Modulate MMP-12 Production via PAR2 and Are Involved in the

423 Long-Term Airway Inflammation and Airway Hyperresponsiveness Induced by  
424 Respiratory Syncytial Virus Infection. *J. Virol.* **90**, 2536-2543 (2015).

425  
426 **Acknowledgments:** We thank Y. Wang for pathological analysis.

427 **Funding:** This work was supported by the Key-Area Research and Development Program of  
428 Guangdong Province (2018B030331001 to L.L.); Shenzhen Science Technology and Innovative  
429 Commission (SZSTI) (SZSTI JCYJ20170307095633450, Research and Application of  
430 Individualized Precise Diagnosis and Treatment Strategies for COPD to L.W.; JCYJ  
431 20180508152336419 to L.L.); Guangdong International Cooperation Grant (2019A050510032 to  
432 KP.L., L.L.); Clinical research of Health and Family Planning Commission of Shenzhen  
433 Municipality (SZLY 2017024 to L.W.); National Natural Science Foundation of China (NSFC  
434 81770028 to C.Q, NSFC 31971072 to L.L.).

435 **Author contributions:** L.W. and L.L. designed the project. K.L performed experiments with S.J.  
436 and Z.L. K.L., S.C., L.L. and L.W analyzed data and prepared the manuscript with inputs from  
437 KP.L. L.W. L.L and C.Q. planned, designed, supervised, and coordinated the overall research  
438 efforts.

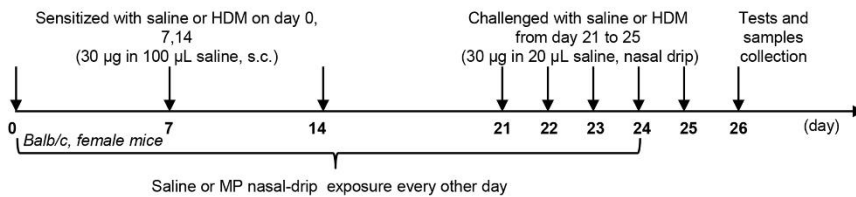
439 **Competing interests:** The authors declare that they have no competing interests.

440 **Data and materials availability:** All data needed to evaluate the conclusions in the paper are  
441 present in the paper and/or the Supplementary Materials. Additional data are available from authors  
442 upon reasonable request.

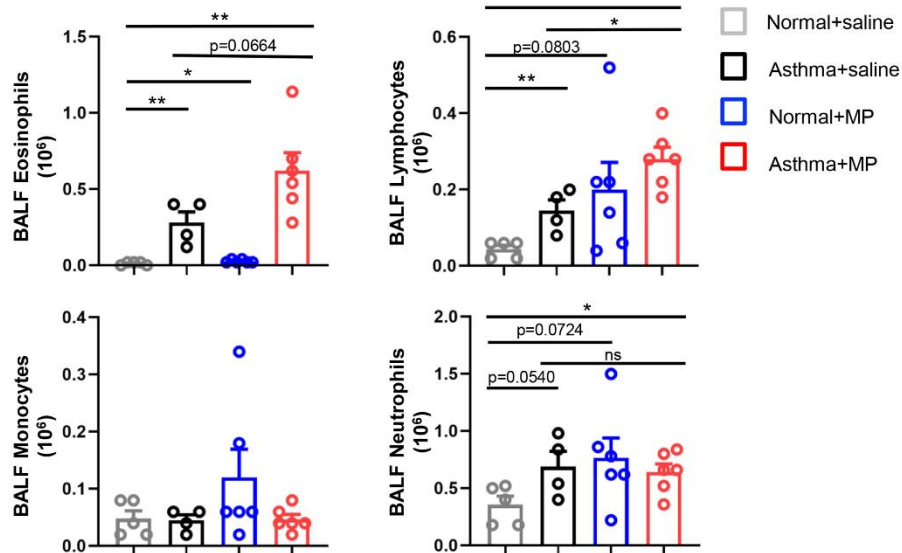
443 **Figures and Tables**

444 **Figure 1**

### A Allergic asthma model and MP treatment



### B



### C

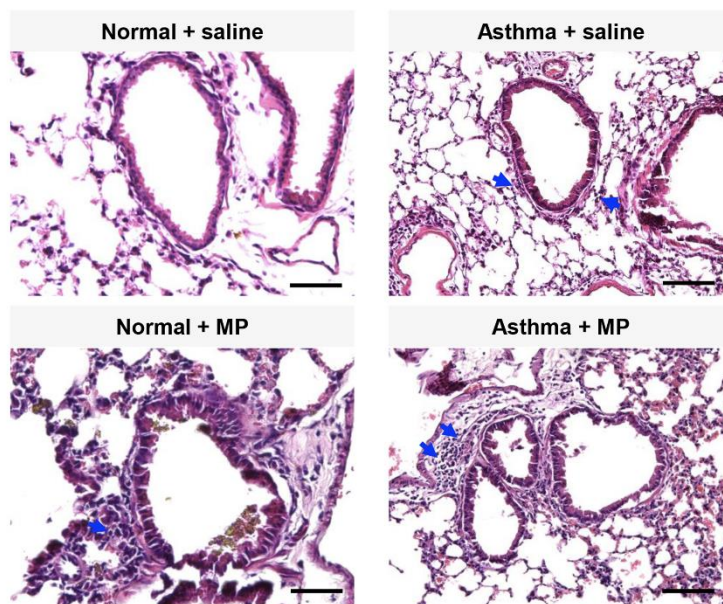


**Fig. 1. Nasal microplastic exposure induces an increase in pulmonary inflammatory cells in normal and asthmatic mice.** (A) Timeline of the allergic asthma model and MP treatment. Four groups were included in the experimental set-up: Normal with saline, HDM-induced asthma with saline, Normal with MP exposure and HDM-induced asthma with MP exposure, s.c., subcutaneous

450 injection. (B) Eosinophils, lymphocytes, monocytes and neutrophils in the bronchoalveolar lavage  
451 fluid (BALF). Results are expressed as mean  $\pm$  S.E.M. n=4~6 per group, each dot represents one  
452 mouse, \* $P < 0.05$ , \*\* $P < 0.01$ , \*\*\* $P < 0.001$ . (C) Representative images showing inflammatory  
453 cell infiltration in the lungs revealed by H&E staining. Arrows: inflammatory cells, scale bars=50  
454  $\mu\text{m}$ , n=4~6 per group.

455

456 **Figure 2**

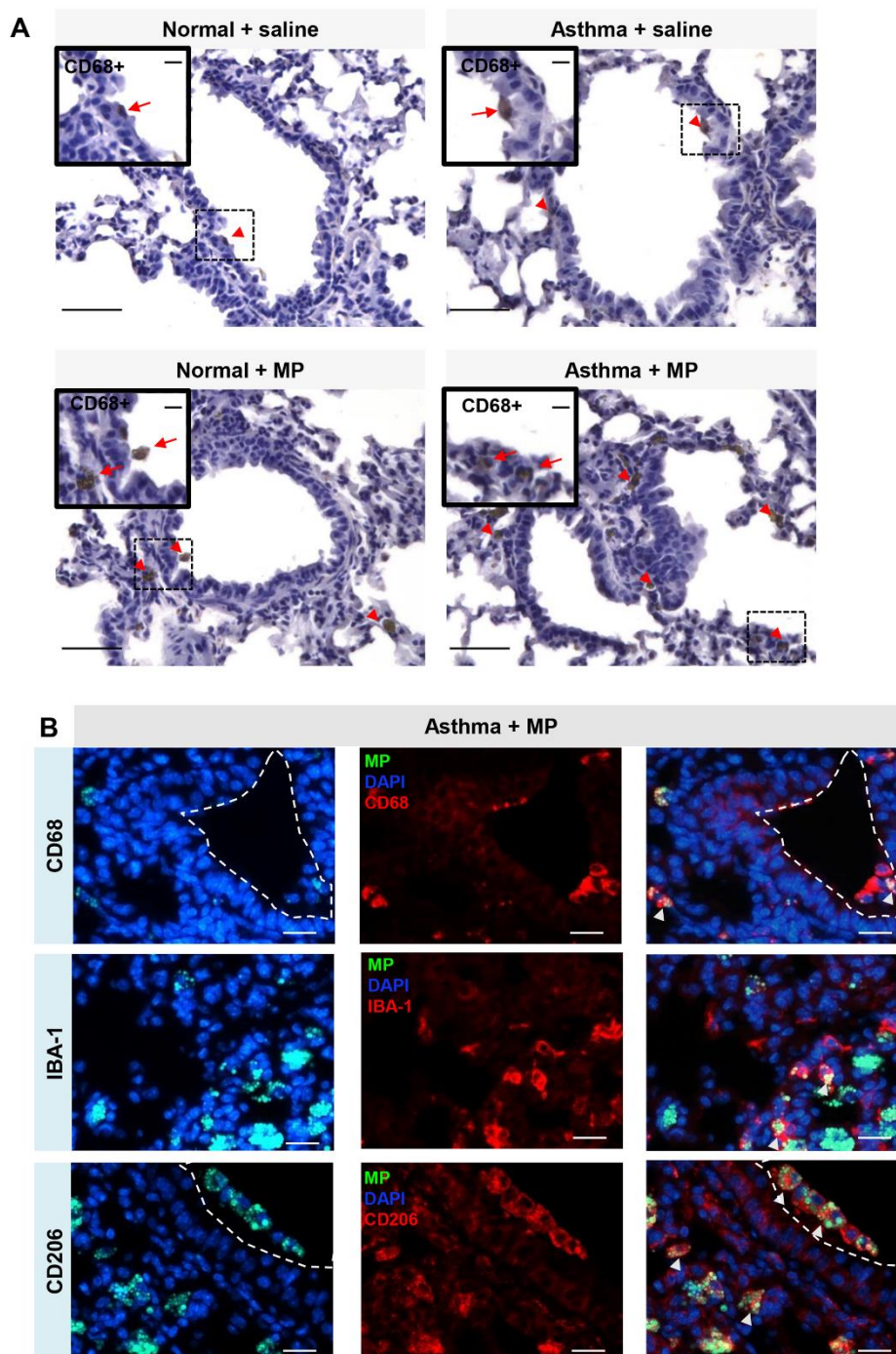


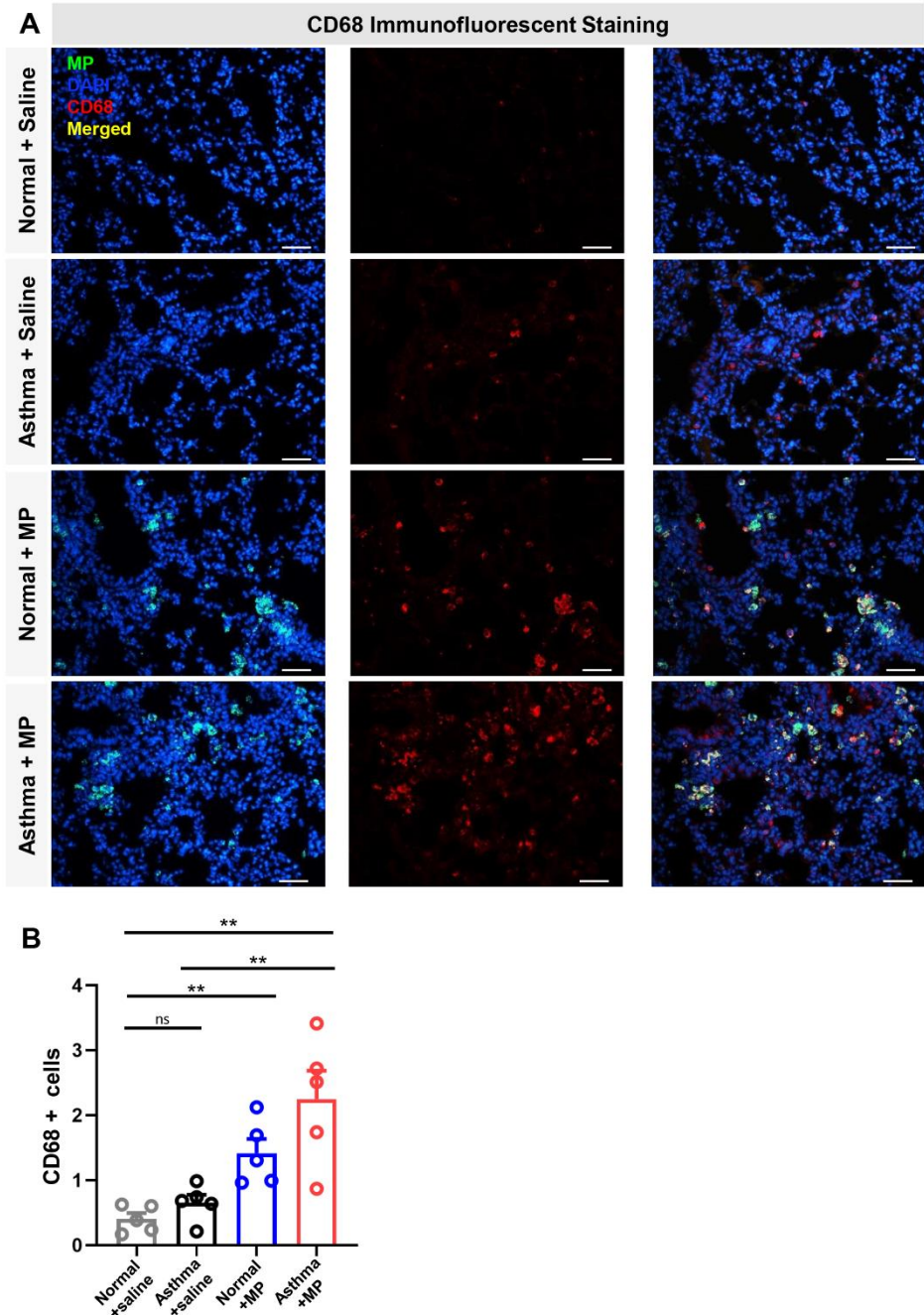
**Fig. 2. MP exposure induces an aggregation of macrophages and phagocytosis of MP particles.**

(A) Photomicrographs showing immunohistochemical staining of macrophage marker CD68 in lung sections. Scale bars, 50  $\mu\text{m}$ , inset scale bars, 10  $\mu\text{m}$ . (B) Photomicrographs showing immunofluorescent staining of macrophages in lung sections of Asthma+MP mice using three markers, CD68, IBA-1 and CD206 (green, MP; blue, DAPI; red, antibody-specific fluorescence;



463 yellow, arrows, merged color showing phagocytized MP particles by macrophages; scale bars, 20  
464  $\mu\text{m}$ ).

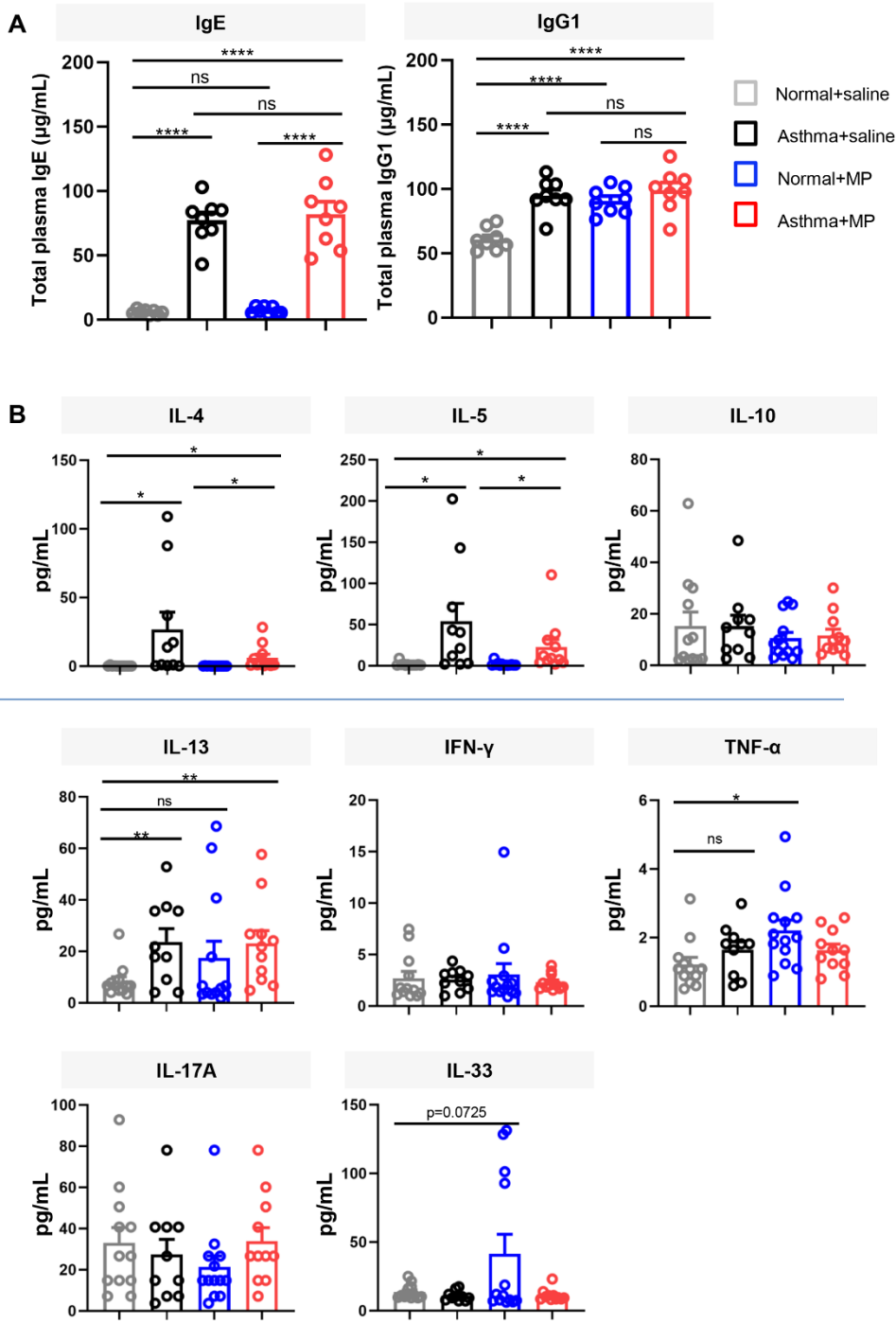
465 **Figure 3**



466  
467 **Fig. 3. Macrophage aggregation induced by MP exposure and quantification across different**  
468 **treatments. (A)** Photomicrographs of macrophages using immunofluorescent staining of CD68 in  
469 lung sections from different treatment groups. Scale bars, 50  $\mu\text{m}$ . **(B)** Quantification of pulmonary  
470 macrophages in different treatment groups. Results are expressed as mean  $\pm$  S.E.M. (n=5 per group).

471 \* $P < 0.05$ , \*\* $P < 0.01$ ; ns, no significant difference, each dot represents the averaged value for one  
 472 mouse.

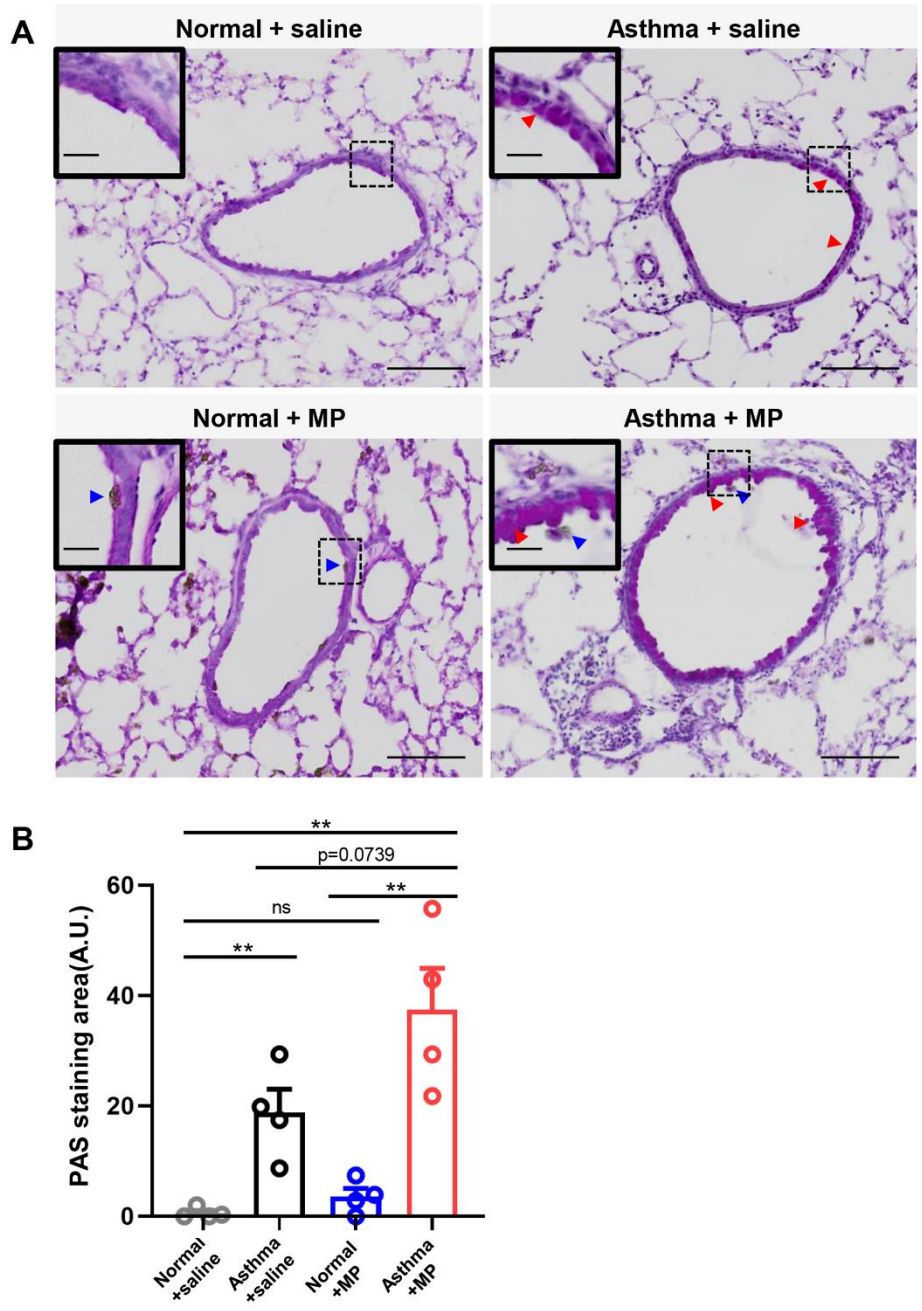
473 **Figure 4**



474  
 475 **Fig. 4. Immunoglobulin and inflammatory cytokine levels in normal and asthmatic mice with**  
 476 **or without MP exposure.** (A) Total IgE and IgG1 levels in plasma. Data are expressed as mean  $\pm$   
 477 S.E.M; n=8 per group, each n represents one mouse; \* $P < 0.05$ , \*\* $P < 0.01$ , \*\*\* $P < 0.001$ , \*\*\*\* $P$

478 < 0.0001. (B) Plasma levels of interleukin (IL)-4, IL-5, IL-10, IL-13, interferon-gamma (IFN- $\gamma$ ),  
 479 tumor necrosis factor-alpha (TNF- $\alpha$ ), IL-17A, and IL-33 in BALF. Data are expressed as mean  $\pm$   
 480 S.E.M; n=10~13 per group, each dot represents one mouse; \* $P$  < 0.05, \*\* $P$  < 0.01.

481 **Figure 5**

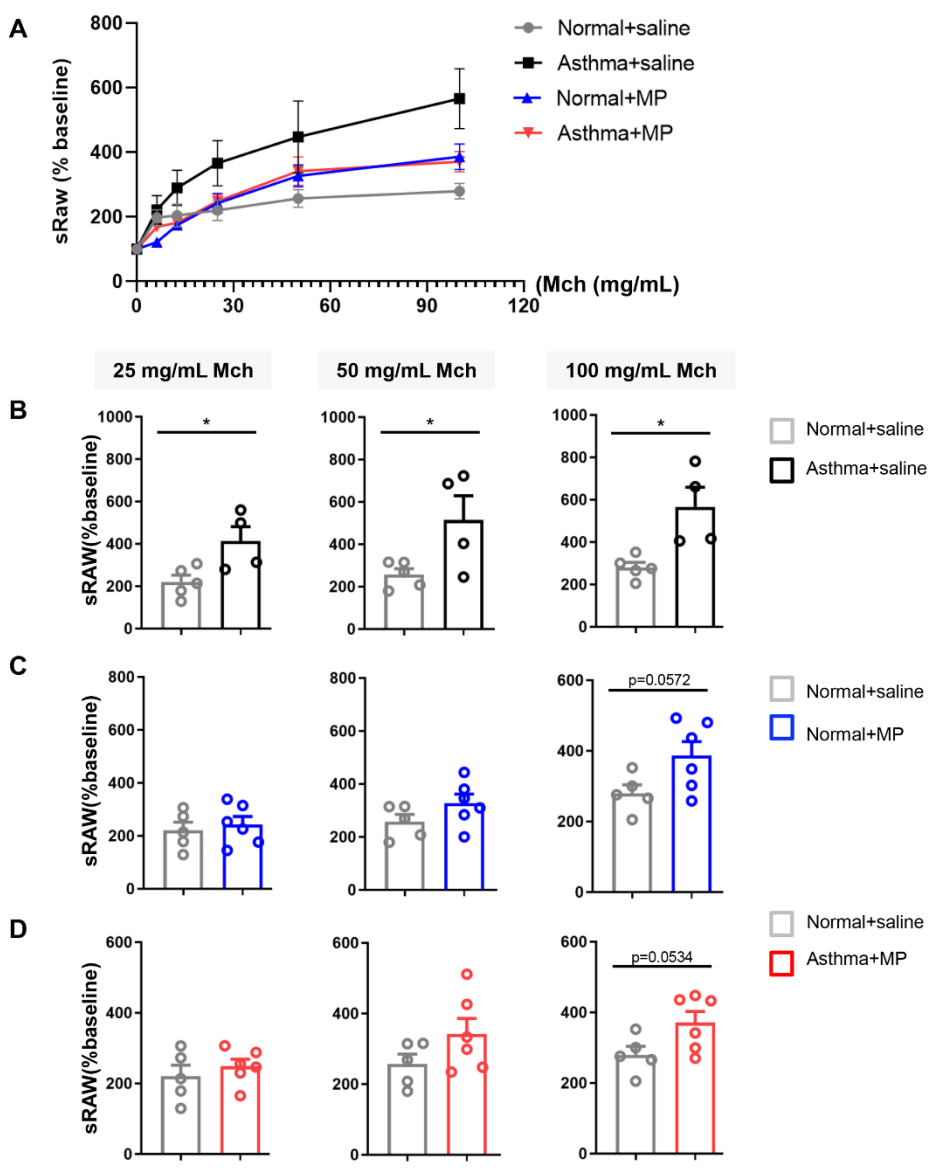


482  
 483 **Fig. 5. The effect of MP exposure and the synergistic effect with asthma on airway mucus**  
 484 **production.** (A) Representative photomicrographs of periodic acid-Schiff (PAS) stained airway  
 485 sections. Epithelial areas in dashed boxes are enlarged in top left insets. Red arrowheads, mucus in



486 airway; blue arrowheads, MP in airway. Scale bars, 100  $\mu$ m; inset scale bars, 20  $\mu$ m. (B)  
 487 Quantification of the mucus production. Data are expressed as mean  $\pm$  S.E.M; n=4 per group, \*\**P*  
 488 < 0.01, each dot represents the averaged value for one mouse.

489 **Figure 6**

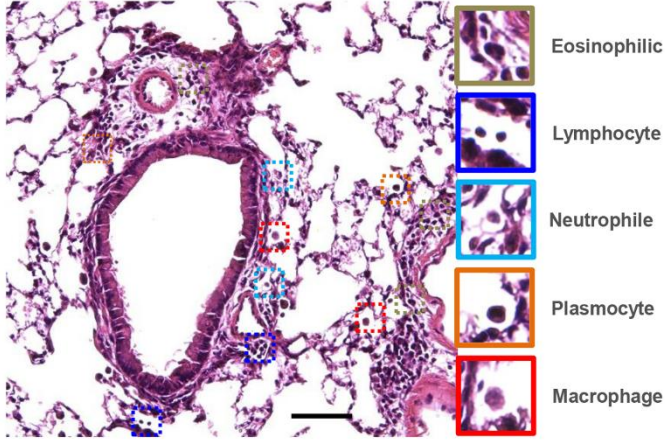


490  
 491 **Fig. 6. MP exposure showed no effect on airway hyperresponsiveness.** (A) Airway response to  
 492 aerosol methacholine in each group. sRAW, special airways resistance. The difference in response  
 493 to methacholine (at concentrations of 100, 50, 25 mg/mL) compared across groups: (B)  
 494 Asthma+saline vs. Normal+saline; (C) Normal+MP vs. Normal+saline; (D) Asthma+MP vs.

495 Normal+saline. Data are expressed as mean  $\pm$  S.E.M. n=4~7 per group, \*P < 0.05; ns, no  
496 significant difference, each dot represents one mouse.

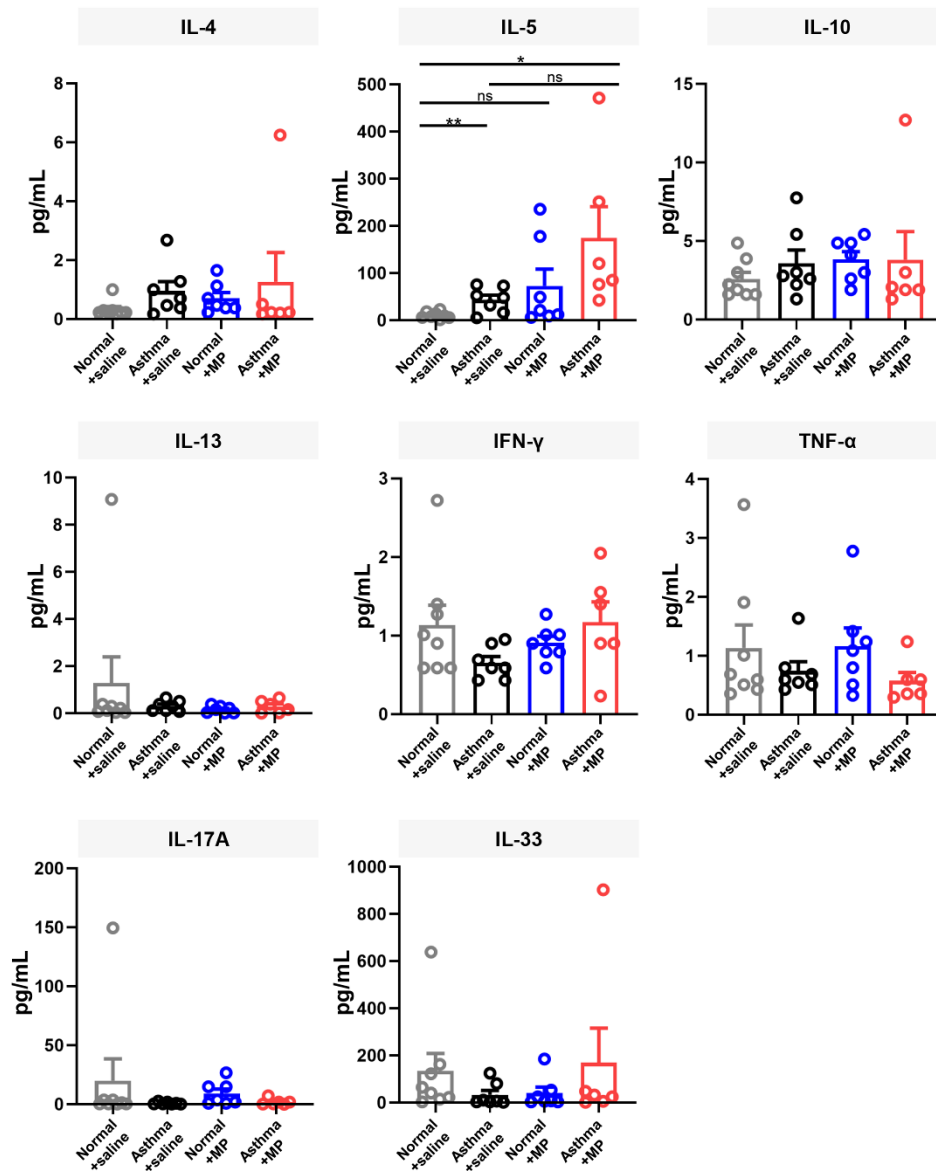
497 **Supplementary Materials**

498 **Figure S1**



499  
500 **Fig. S1 Representative H&E staining showing infiltration of different inflammatory cells in**  
501 **the lung.** The dashed squares are enlarged on the right to show the histological features present in  
502 eosinophils, lymphocytes, neutrophils, plasmocytes and macrophages. Scale bar, 50  $\mu$ m.

503 **Figure S2**



504  
505 **Fig. S2 Plasma cytokine levels of normal and asthmatic mice with or without MP exposure.**

506 Plasma levels of interleukin (IL)-4, IL-5, IL-10, IL-13, IFN- $\gamma$ , TNF- $\alpha$ , IL-17A and IL-33 in each  
507 treatment group. Data are expressed as mean  $\pm$  S.E.M; n=6~8 per group. \* $P < 0.05$ , \*\* $P < 0.01$ ,  
508 each dot represents one mouse.

509 **Graphical Abstract**

